Supplemental figures

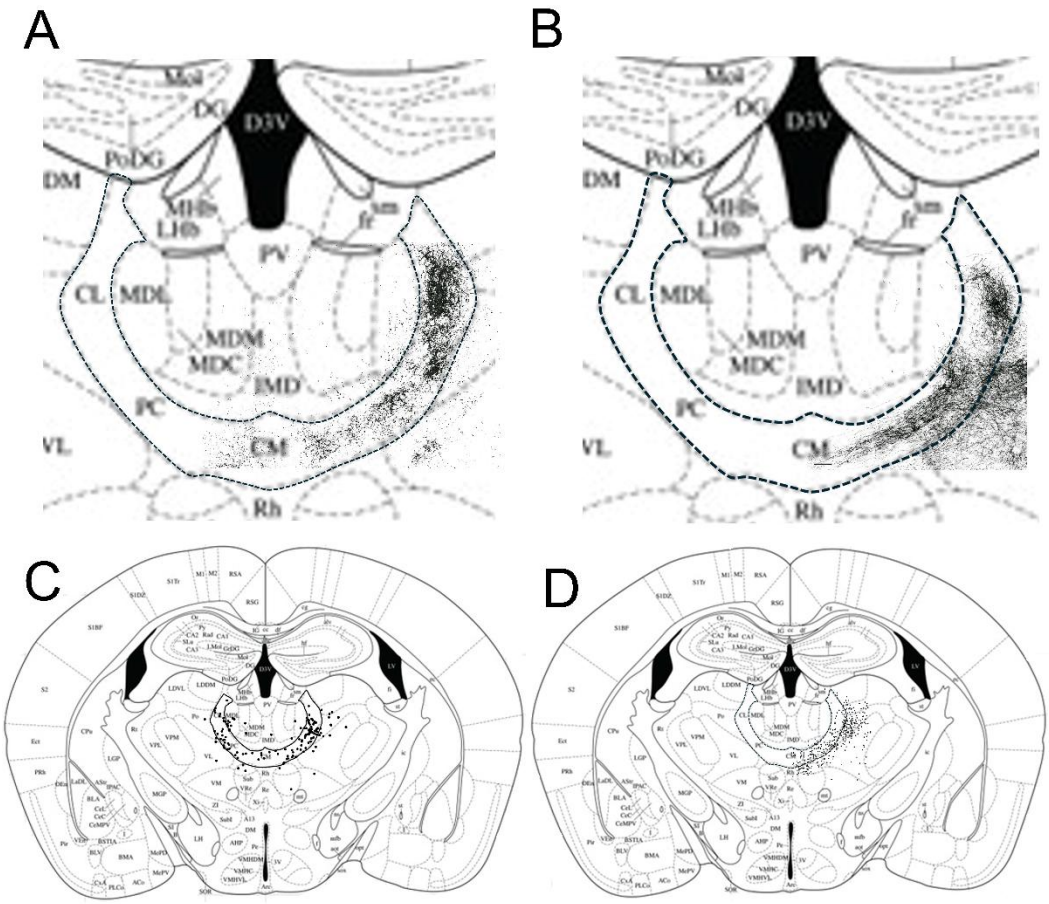

Supplementary Figure 1: Location of the CL nucleus relative to projections, recorded neurons, and tectorecipient cells investigated in the study. Confocal images of Pitx2 SC (A) and motor cortex (B) projections, plots of neurons recorded in brain slices (C) and location of tectorecipient neurons labeled via transsynaptic viral tracing (D) overlaid on Paxinos mouse brain atlas sections (1.31mm posterior to Bregma).

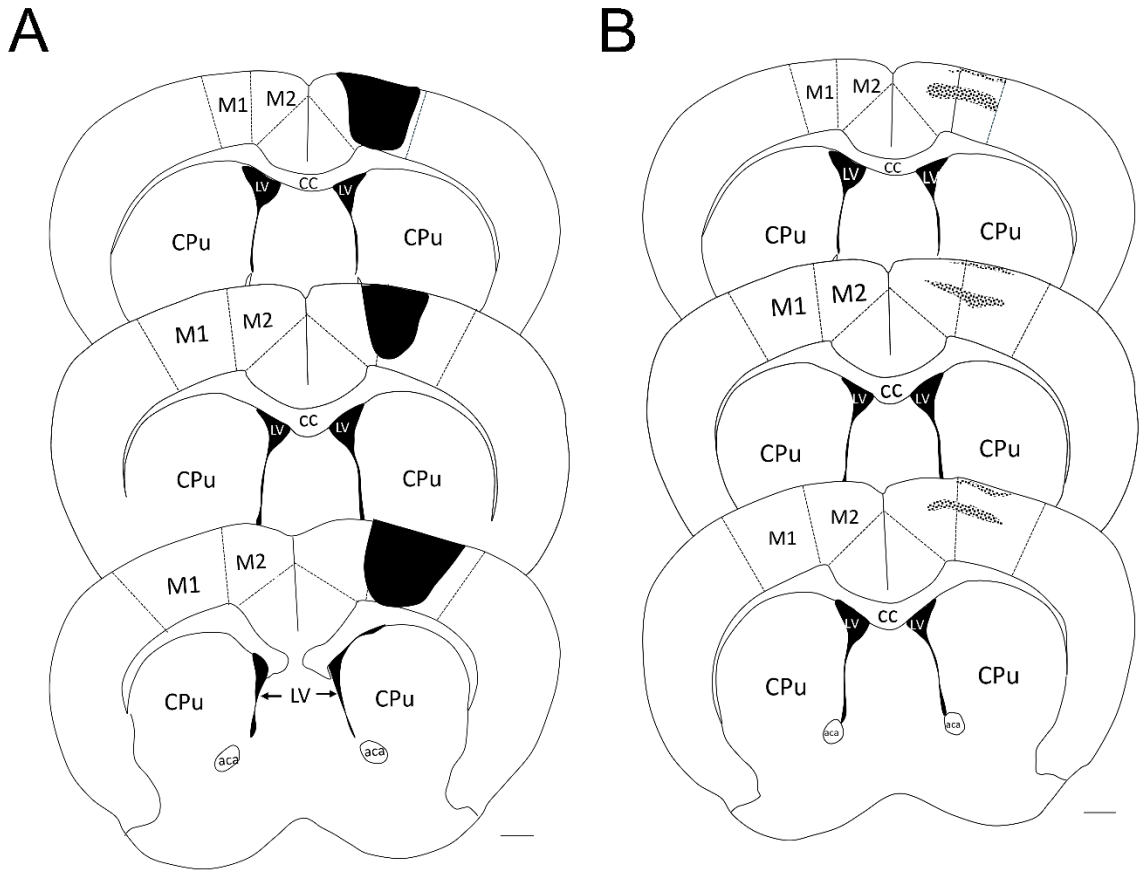

Supplementary Figure 2: Schematics of injection sites in the motor cortex (A, black, see also Figure 1D (inset) and projections from the tectorecipient CL nucleus to the motor cortex (B, black stipple, see also Figure 1I) plotted based on confocal images of experimental tissue. Scale bars: 100µm.

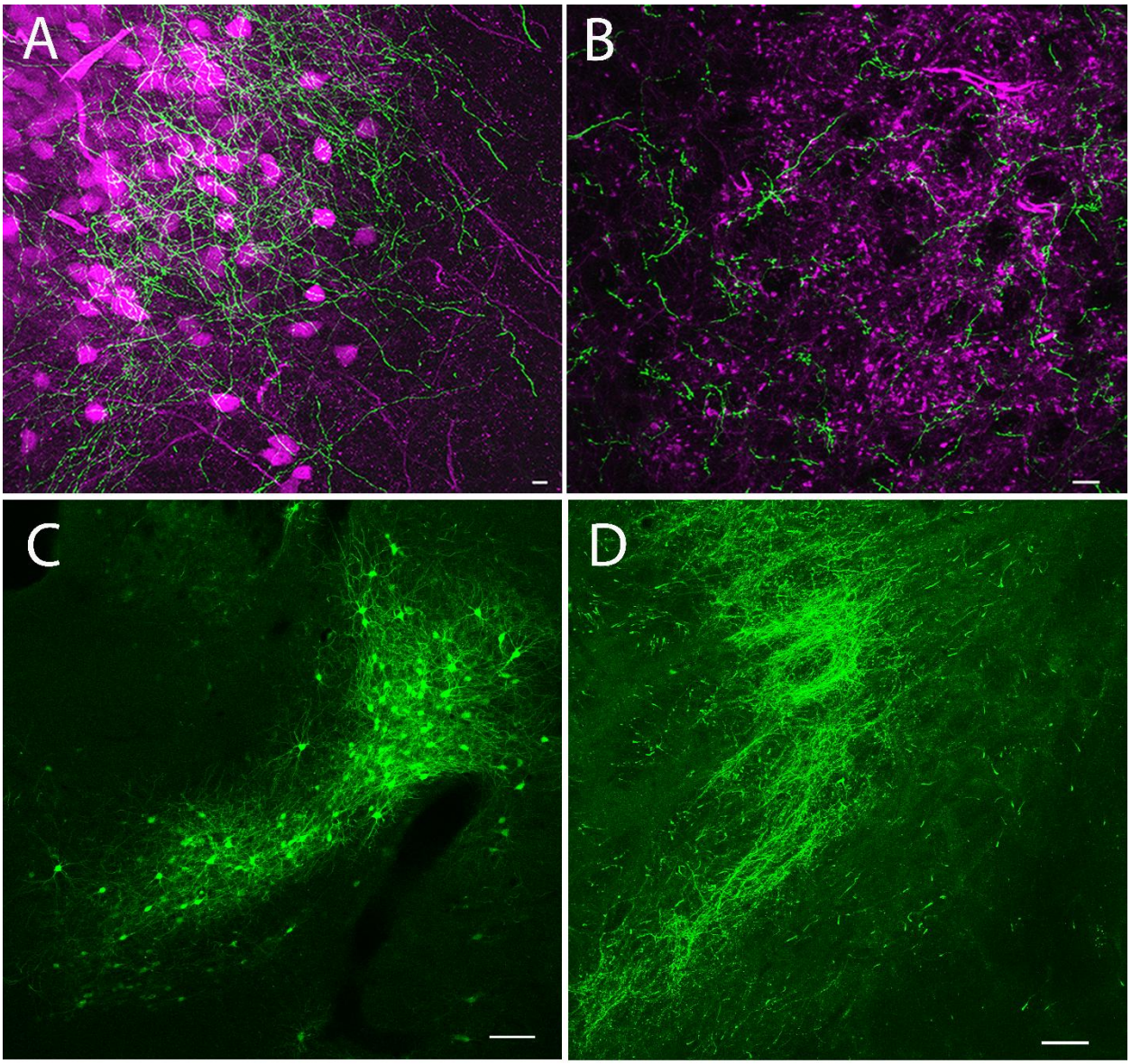

Supplementary Figure 3: A, B) The motor cortex (MCtx) of a Pitx2-Ai9 mouse was injected with a virus to induce the expression of EYFP. MCtx terminals (green) surround Pitx2 cells (magenta) in the SC (A) and MCtx (green) and Pitx2 (magenta) terminals overlap in the CL nucleus (B). C, D) Tectorecipient CL cells and projections labeled via transsynaptic virus tracing. An example of a single (5 um) optical section of labeled tectorecipient CL cells (C) and projections of tectorecipient CL cells to the thalamic reticular nucleus (D). Scale bar in A and D: 50μm and in B: 20 μm, in C: 100 μm.

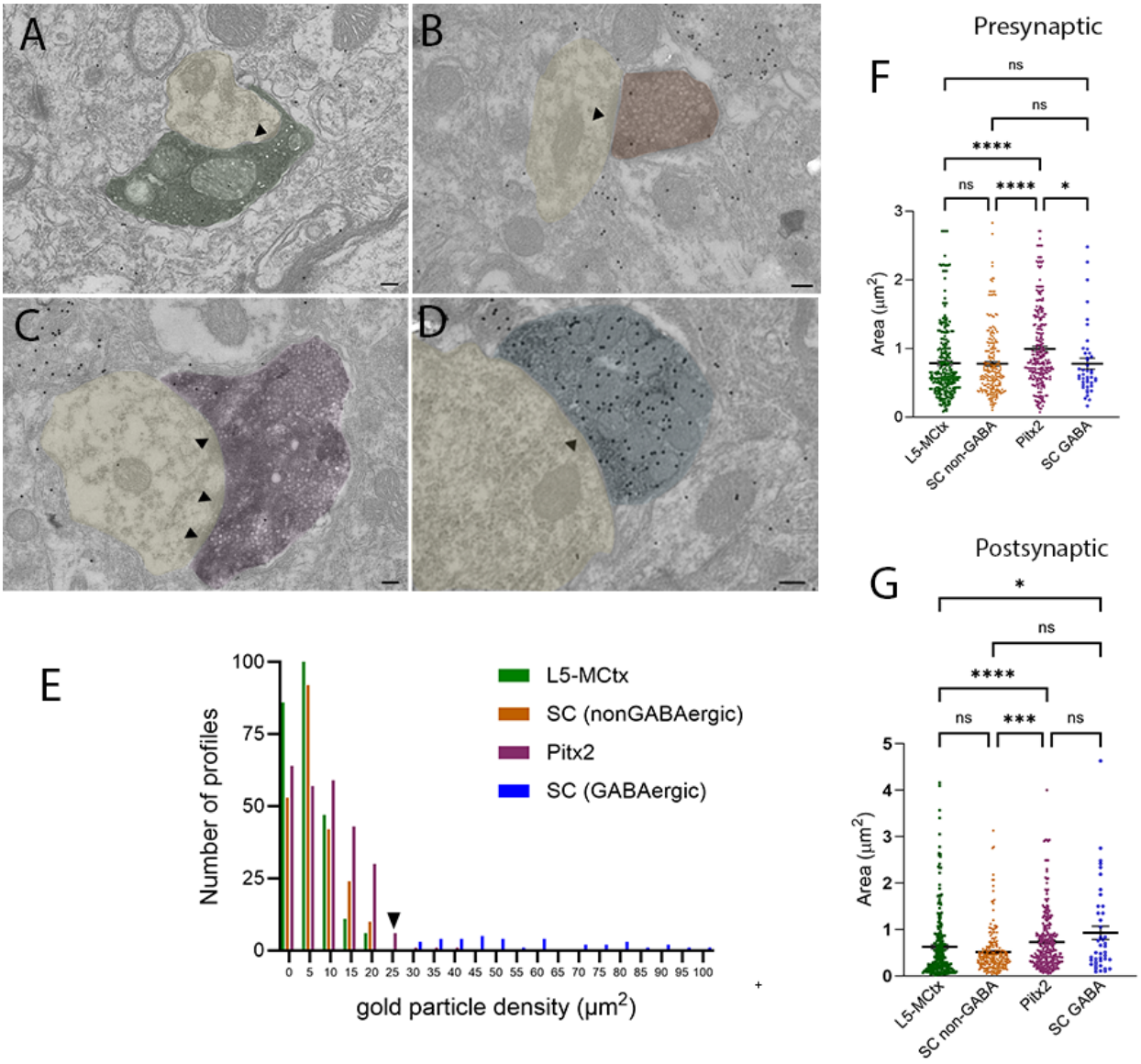

Supplementary Figure 4: A-D) Example images of labeled L5-MCtx (A, green overlay) nonGABAergic SC (B, orange overlay) Pitx2 (C, purple overlay), and GABAergic SC synaptic terminals (D, blue overlay). Synapses are indicated with black arrowheads and postsynaptic dendrites and indicated with yellow overlays. E) Frequency distribution of the density of gold particles overlying L5-MCtx (green bars), SC (orange and blue bars), and Pitx2 terminals (purple bars). We used the average + 2X the standard deviation of

the gold particle density overlying Pitx2 terminals as the cutoff value for determining GABAergic (>24 gold particles/um^2) vs nonGABAergic (<24 gold particles/um^2) profiles in the CL (indicated by the black arrowhead). F, G) Comparison of the sizes of presynaptic profiles (F) and their postsynaptic targets (G). Presynaptic Pitx2 terminals are significantly larger than L5-MCtx ($p<0.0001$), nonGABAergic SC ($p<0.0001$), and GABAergic SC ($p=0.0364$) terminals in the CL. G) The postsynaptic dendritic partners of Pitx2 terminals were significantly larger than those postsynaptic to L5- MCtx ($p<0.0001$) and nonGABAergic SC (0.0002) terminals, but not GABAergic SC terminals ($p>0.9999$). Kruskal-Wallis test was used for statistical analysis and shown are the mean and standard errors of the mean. Scale bars: 300nm (A, B, C, D). Color code in E applies to all panels.

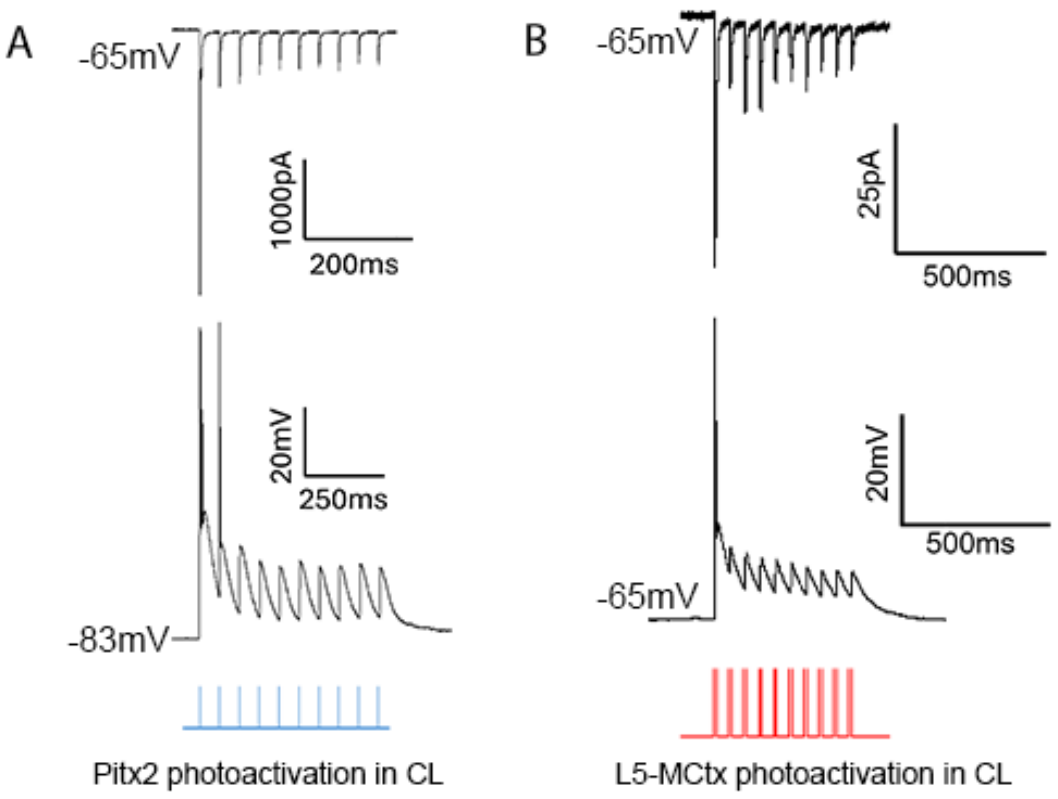

Supplementary Figure 5: A) Photoactivation of Pitx2 terminals (light pulses shown as blue ticks) occasionally elicited action potentials in response to the first light pulse (n=4) and were visible in both voltage (top trace) and current (bottom trace) clamp; these were excluded from the analysis of frequency-dependent response and comparison of response amplitude in Figures 3D and 5. B) The photoactivation of L5-MCtx terminals (light pulses shown as red ticks) also occasionally generated action potentials in postsynaptic CL neurons (n=3) that were visible in both voltage (top trace) and current (bottom trace) clamp; these were excluded from the analysis of frequency-dependent response and comparison of response amplitude in Figures 4D and 5.

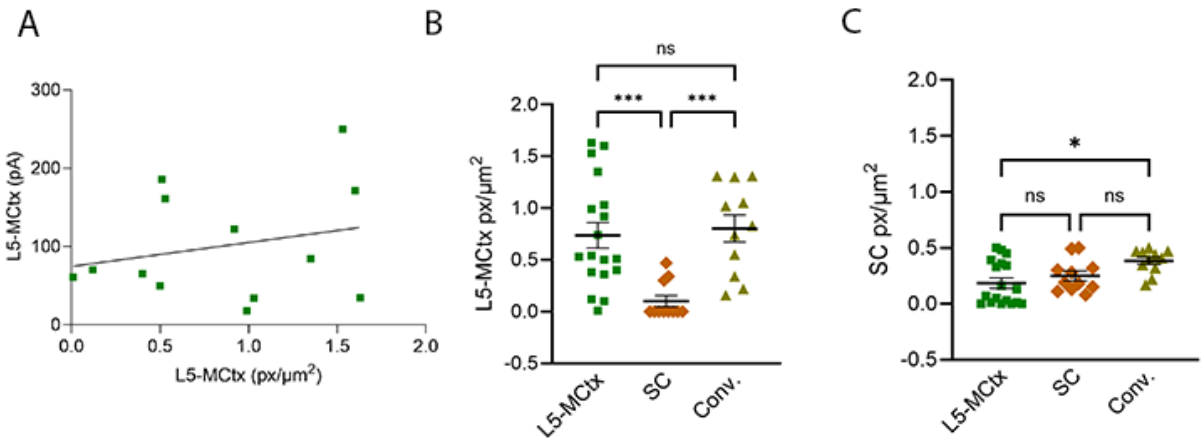

Supplementary Figure 6: A) Non-linear curve fitting regression analysis of response amplitudes vs pixel densities for CL cells that responded to photoactivation of L5-MCtx terminals. There is a trend for increased EPSC amplitude with increased terminal density around the CL cells. B) Comparison of the densities of L5-MCtx terminals surrounding CL cells that responded to SC only, L5-MCtx only, or both SC and L5-MCtx (conv). Statistical analysis showed a significant difference in pixel densities surrounding cells that responded to L5-MCtx only or SC only ($p=0.0004$) but not between those that responded to L5-MCtx only or L5-MCtx and SC ($p>0.9999$). C) Comparison of the densities of SC terminals surrounding CL cells that responded to SC only, L5-MCtx only, or L5-MCtx+SC (conv). Statistical analysis showed a significant difference in SC pixel densities surrounding cells that responded to L5-MCtx only or L5-MCtx and SC

(p=0.0122) but not between those that responded to SC versus conv. (p=0.2740) or SC versus L5-MCtx (p=0.9645). Kruskal-Wallis test was used in B and C.

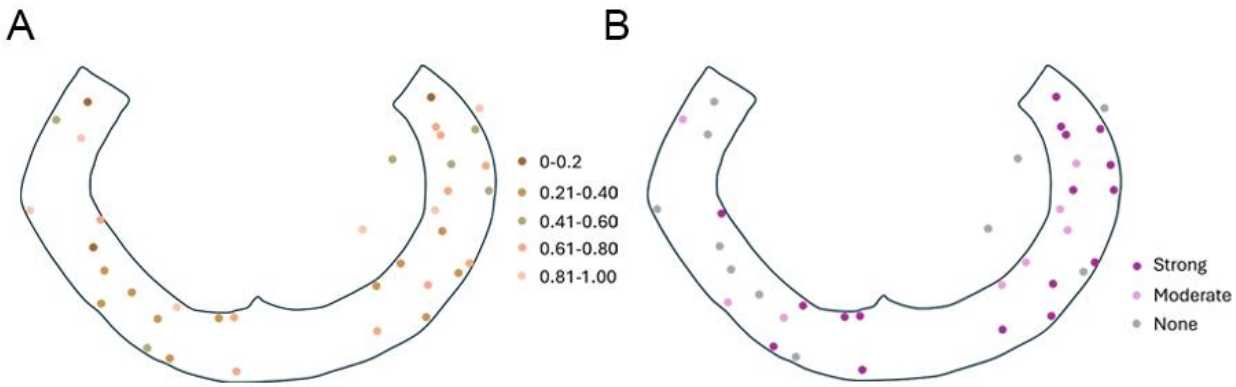

Supplementary Figure 7: A) Location of CL cells responsive to optogenetic activation of Pitx2 terminals; dots are color coded to indicate their dendritic orientation indices (DO*i*). B) The same cells plotted in A are shown with the color of dots coded to indicate response strength.

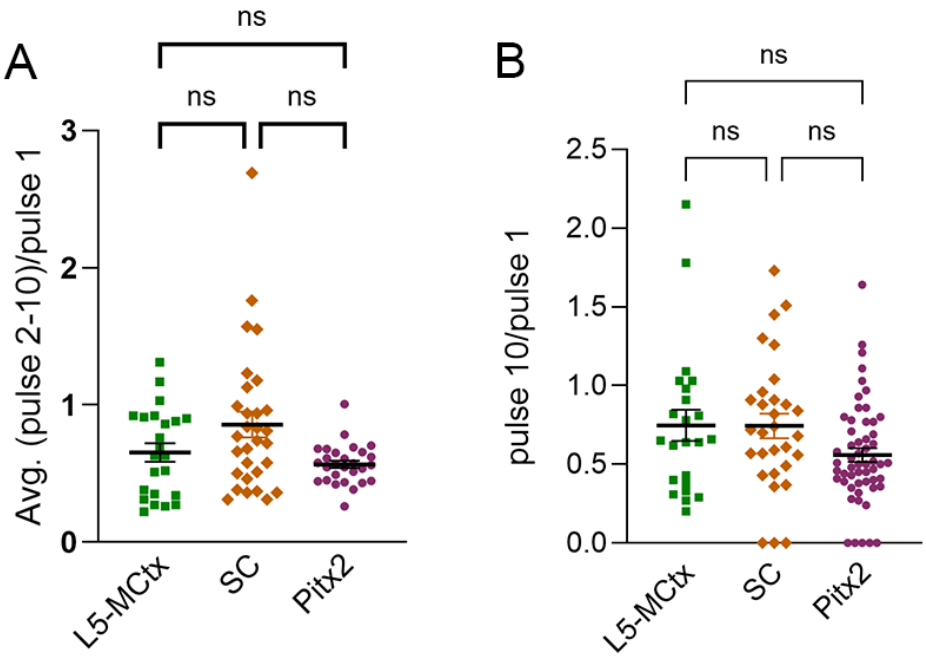

Supplementary Figure 8: A) The average response amplitudes to pulses 2-10 of a 20Hz train divided by the amplitude of the response to pulse 1 for each CL cell that

responded strongly or moderately to the photoactivation of L5-MCtx (n=23), SC (n=30) or Pitx2 (n=55) terminals. We found no significant difference in the frequency-dependence of L5-MCtx vs SC ($p=0.4817$), L5-MCtx vs Pitx2 ($p>0.9999$), or SC vs Pitx2 ($p=0.1236$) responses. B) We found no significant differences in the frequency-dependence of CL cells to pulse 10 divided by the response amplitude to pulse among photoactivated L5-MCtx, SC, or Pitx2 terminals. L5-MCtx vs SC ($p>0.9999$), L5-MCtx vs Pitx2 ($p=0.3749$), or SC vs Pitx2 ($p=0.0743$) responses.